

Analysis of Seam Weld Strength and Micro Structural Properties of Welded Dual Phase Steel Tubes

A. Sudheer, S. Jose

Abstract- Welded steel tubes of advanced high strength category are considered as candidate material for replacing the drive shafts in automobiles. Seam welded Dual phase steel tubes of various grades were tested to analyze their strength and compatibility to replace drive shaft in light motor vehicles. The tensional fatigue life was found to be varying for specimens with varying test conditions. In all cases, failure was found to occur at the welded region of tubes in longitudinal direction followed by circumferential branching. Failure patterns of each specimen are closely observed under SEM. Fractographs showed clear indications of crack initiation and crack propagation. Energy Dispersive Spectrometry (EDS) analysis were conducted which indicated the impurity concentrations at crack region. Micro structural analysis and hardness measurements of various specimens were carried out along the weld section which clearly showed in homogeneity between base metal and the weld section. Grain size measurements were also done for weld region and base metal.

Keywords: Welded, compatibility, (EDS), Energy, SEM.

I. INTRODUCTION

Dual Phase steels comes under the class of advanced high strength steels (AHSS) and are produced by controlled cooling from the austenite phase (in hot-rolled products) or from the two-phase ferrite plus austenite phase (for continuously annealed cold-rolled and hot-dip coated products) to transform some austenite to ferrite before a rapid cooling transforms the remaining austenite to martensite[1].

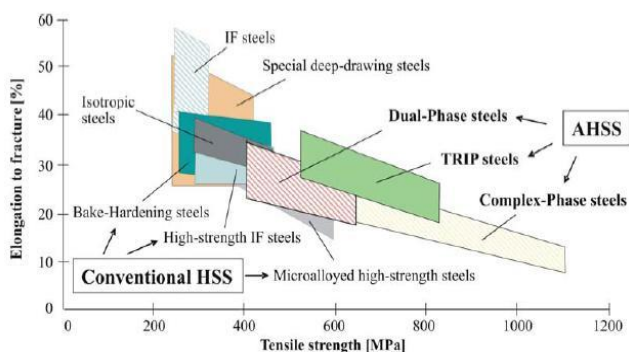


Fig.1 Steel types [2]

DP steel contains ferrite plus islands of martensite. The soft ferrite phase is generally continuous, giving these steels excellent ductility. When these steels deform, strain is concentrated in the lower-strength ferrite phase surrounding the islands of martensite, creating the unique high work hardening rate exhibited by these steels. The work hardening rate plus excellent elongation give DP steels much higher ultimate tensile strengths than conventional steels of similar yield strength.(Fig.2) The DP steel exhibits higher initial work hardening rate, higher ultimate tensile strength, and lower YS/TS ratio than the similar yield strength HSLA steels[3,4].

High frequency (HF) welding is most widely used in the manufacture of longitudinally welded tubes and pipes. In this process, strip material is formed continuously into a tube in a special mill. As the strip edges come together in a V, high frequency current is introduced either by sliding contacts on the tube surface (HF contact) or an HF induction coil around the tube (HFI). Current is concentrated along the edges of the V and provides sufficient local resistance heating on the edges that a weld is formed when squeeze rolls close the tube. Because of the nature of high frequency electrical currents, a physical phenomenon called the “Proximity Effect” forces most of the current to flow on the strip’s edges. This causes the edges to heat to the forge welding temperature and a set of “squeeze” rolls force the edges together under sufficient pressure to produce a forge weld. The weld is a solid phase forge weld with any melted metal and contaminants being displaced into a small upset or bead. This bead is normally scarfed from the tube while hot, immediately after the squeeze rolls(fig.3). The result is, that while the weld is a forge weld with no “cast” structure, the metallurgical properties in the Heat Affected Zone (HAZ) are now different than those of the rest of the pipe[5,6].

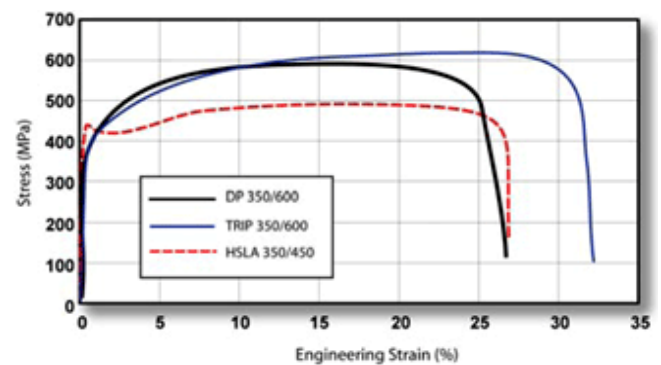


Fig.2 Stress-Strain Curves for HSLA, DP and TRIP Steels. (350 MPa Yield Strength) [2]

Manuscript published on 30 August 2017.

* Correspondence Author (s)

A. Sudheer, Research Scholar, Department of Mechanical Engineering, Faculty of Engineering and Technology, University of Kerala, (Kerala)-695034, India.

S. Jose, Associate Professor, Department of Mechanical Engineering, T.K.M. College of Engineering, Kollam, (Kerala)-695034, India.

© The Authors. Published by Blue Eyes Intelligence Engineering and Sciences Publication (BEIESP). This is an open access article under the CC-BY-NC-ND license <http://creativecommons.org/licenses/by-nc-nd/4.0/>

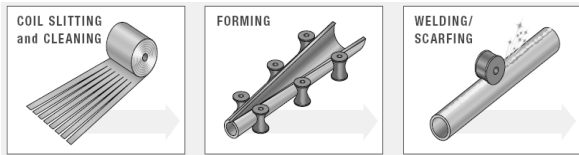


Fig.3 Schematic representation of tube forming and welding process

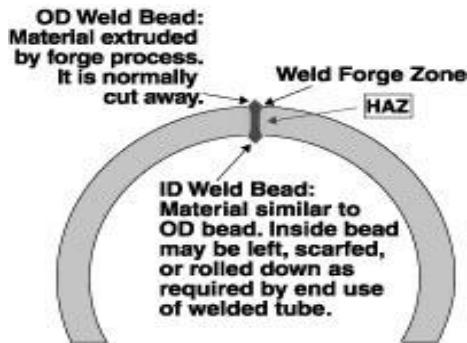


Fig.4 Schematic representation of Pipe section showing Weld Forge Zone, HAZ, and Weld Beads on inner and outer diameter [6]

The fatigue fracture surface is usually brittle-like in form even in ductile materials and is often characterized by striations or beach marks that are formed during crack growth. The applied cyclic stress state may be axial (tension-compression), flexural (bending), torsional (twisting), or a combination of these. The cyclic stress may alternate with a zero mean level, alternate about a mean level, or vary quite randomly with amplitude and frequency[7,8]. A fatigue crack will generally initiate on a free surface at a location of stress concentration through microcracks created during plastic deformation at matrix inhomogeneities (inclusions, grain boundaries). If such microcracks are advantageously oriented, they will be enlarged by the cyclic torsional loading [9].

II. MATERIALS USED FOR ANALYSIS

Steel tube of SAE 1012 grade was the material used for failure analysis. Several tube samples were made with various heat treatment conditions as given in the table 1.

TABLE1. Treatment Conditions Applied for SAE1012 Steel

Material	Conditions			
SAE 1012	As Drawn	DP treated at 740°C and induction tempered at 200°C	DP treated at 780°C and induction tempered at 200°C	DP treated at 800°C and induction tempered at 200°C

III. EXPERIMENTAL PROCEDURES

A. Torsional Fatigue Tests

The torsion testing of tubes was carried out in a Torsion test rig at Tube Products India Ltd., Avadi, for SAE 1012 steel grade for as drawn and DP treated conditions. The length of the specimen used was 750 mm and the gauge

length (grip to grip length) was 530mm with outer diameter, 45 mm and thickness 2.29mm. The torque applied was 1.28 kNm and frequency of 0.75 Hz.

B. Hardness Tests

Hardness tests were carried out on DP treated and as drawn samples prepared from tubes. The specimen was first cut and polished for macro etching to identify the weld section, and an arc shaped portion which includes the weld is polished and etched using 2% Nital, and then taken to the micro hardness tester. Vickers hardness numbers for a load of 500 grams are obtained for weld, HAZ and base metal regions.

C. Optical Microscopy

Optical microscopy was carried out on all types of samples in as drawn and DP treated conditions. The samples are cut to the required sizes from the tube using an electric cutter and were ground and polished in an auto polisher and then in a diamond disc polishing machine. The polished samples were etched with 2% Nital and observed in an optical microscope for magnifications 50X to 500X and relevant photographs were taken.

D. Scanning Electron Microscopy

The torsion tested samples were cut carefully with a hand saw by fixing the pipe in a bench vise without damaging the fracture surface. The cut specimen were ultrasonically cleaned to get rid of oil or dirt and numbered using a scriber along the side of fracture surface for careful observation under scanning electron Microscope. SEM fraction graphs of samples for different magnifications ranging from 25X to 3500X were obtained. Energy Dispersive Spectrometry (EDS) analysis were also done along with this to find the composition of any inclusions found on the surface.

IV. RESULTS AND DISCUSSION

A. Torsional Fatigue Test

Test parameters: Sample size: 750 mm (L) X 45.06 mm (OD) X 2.29mm (T), Gauge length: 530 mm, Torque applied: 1.28 kNm, Calculated shear stress: 205 MPa , Frequency: 0.75 Hz

Table 2: Fatigue Test Results

condition	sample	Cycles To failure	Hardness (VHN)		remarks	
			weld	base		
As drawn	AS1	23000	200	205	Failed Along weld	
	AS2	25000				
	AS3	23300				
DP Treatment Temp	740	BS1	219	251	Failed Along weld	
		BS2				18200
		BS3				6500
	780	CS1	14775	196	216	Failed Along weld
		CS2	5029			
		CS3	6680			
	DS1	8103			Failed	



(°C)	810	DS2	6296	216	251	Along weld
		DS3	8523			

The tested specimens had cracks in longitudinal direction which has branched circumferentially on both ends of longitudinal crack. The first attempts were to find any correlation between the longitudinal crack length of failed samples and its fatigue life, but couldn't get a linear relation.

The data from table clearly shows better results for SAE1012 as drawn samples which consistently clocked above the 23000 cycles.(Table2) Micro hardness test conducted in the base metal and the weld section clearly showed difference in hardness in the two regions of all samples. But the difference in hardness value was the least in this case. Hardness values of as drawn condition is less compared to the DP treated ones, but it has more homogeneity in structure. Although DP treatment was expected to increase the homogeneity between the weld and base metal it was found that the hardness difference has increased with more martensitic concentration at the base metal and very low martensitic concentration at weld region.

B. SEM Analysis

The cut specimens for SEM observation are shown in Fig.5. General observations clearly indicated that the crack has initiated in the longitudinal part of fracture surface and grown to a certain length, and then branched circumferentially. This pattern was similar for all specimens except for the variation in the longitudinal crack length along the weld line. Careful observations in SEM has helped to identify the fracture initiation points in the fracture surface.



Fig.5 Cut specimens for fracture surface observations under SEM

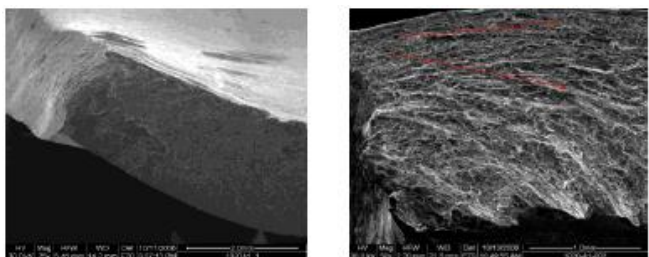


Fig 6. Tip of the fracture surface Fig 7. Crack initiation site

Fracture surface observation under SEM for magnification of 25X (as shown in Fig.6) throughout the longitudinal crack length showed some specific patterns indicative of fracture initiation regions. One or more initiation regions were found in all cases, and these regions were subjected to higher magnifications in the order of 800X to 3000X under SEM. The Fig.7 shows a fracture initiation region at one end of longitudinal fracture surface of SAE1020 as drawn sample. In this case the crack branching point itself shows a

crack initiation site while other specimens showed crack initiation near to weld region at mid portion of the test specimen. The Fig.8 shows another fracture initiation region near the centre portion of the longitudinal fracture surface. This centre portion was found in a slight bluish coloration similar to a heat affected zone. This region also appears smooth and sharp compared to other regions. These features are indicative of a brittle type of fracture initiation and further fast propagation through the weld line before it gets branched circumferentially and then the material fails. Also the centre portions in these case appeared smooth compared to adjacent parts which is due to the rubbing action during cyclic loading between the mating surfaces in the weld region.

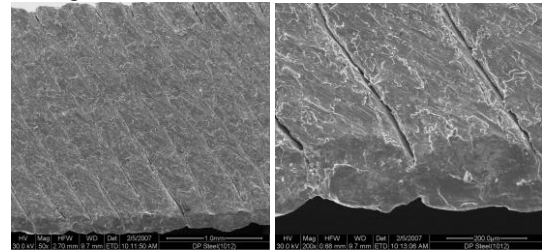


Fig 8. Fracture surface of SAE1012M DP@740°C showing crack formation in torsional loading direction

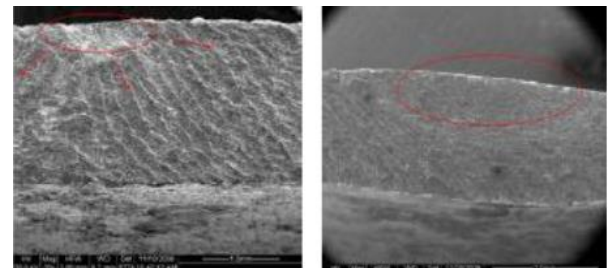


Fig.9. Outer edges of fracture surface showing possible crack initiation sites

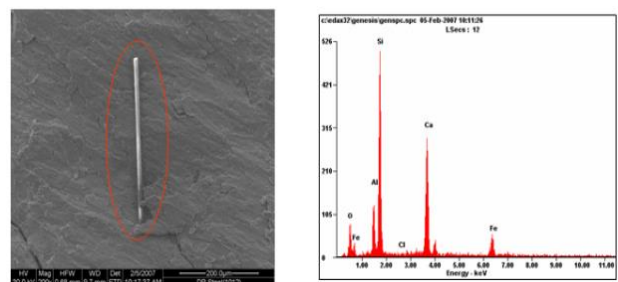


Fig 10. Needle like impurity as seen in fracture surface of SAE1012M DP@740°C sample failed at 6500 cycles.

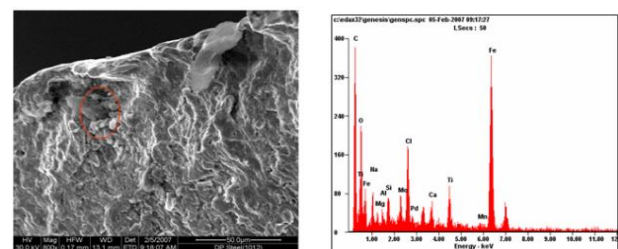


Fig 11. Impurities as seen in fracture surface of SAE 1012 M As drawn

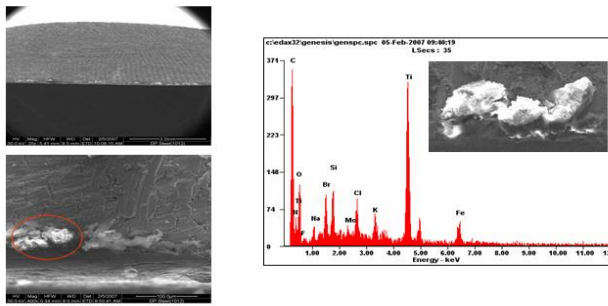


Fig 12. Ti impurities as seen in fracture surface of SAE1012M DP@740°C sample failed at 6500 cycles. Ti impurity is generally more in this grade

The SEM fractographs and EDS analysis were indicative of the following

1. The crack initiation has occurred in the outer edge of the longitudinal weld region.
2. In most cases the crack has originated near the centre of the longitudinal weld region and propagated towards both sides where it branches circumferentially.
3. The fracture is initiated through micro crack formation which eventually grows and leads to failure.
4. The crack has always initiated near some impurities or inclusions which mainly included Calcium or Aluminum silicates and oxides.
5. Fatigue striations (indicative of fatigue fracture) were observed invariably in all specimens.

C. Microstructural Analysis

SAE1012 microstructures corresponding to various test conditions were obtained in metallurgical microscope for base metal and weld section.

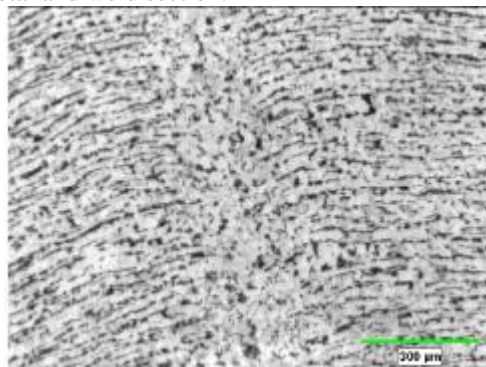


Fig 13. Microstructure of SAE 1012 As drawn Sample near weld region

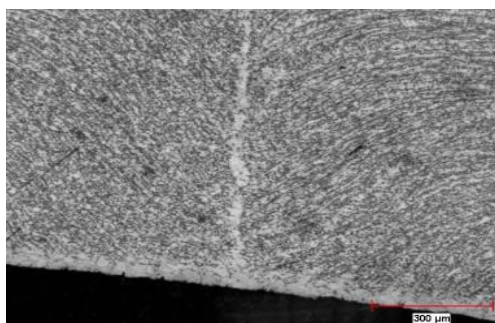


Fig14 (a). Microstructure of SAE 1012 DP @ 740°C and induction tempered at 200°C for 1h showing decarburization at weld and surface

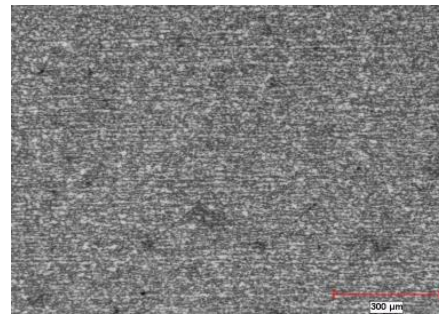


Fig. 14(b) Base metal microstructure of SAE 1012 DP @ 740°C

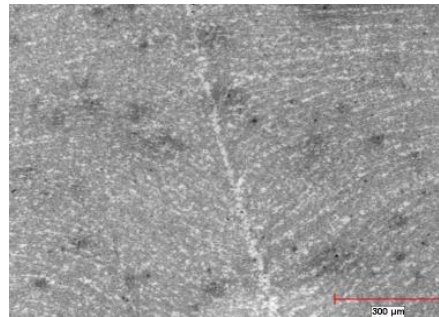


Fig.15 (a) Microstructure of SAE 1012 DP @ 800°C and induction tempered at 200°C for 1h (near weld region)

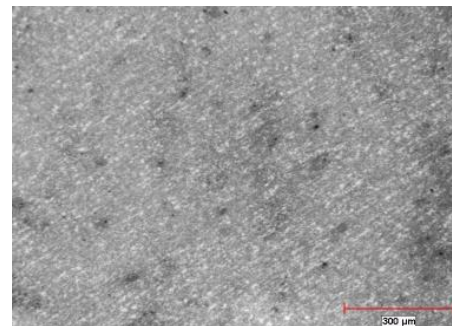


Fig.15 (b) Microstructure of SAE 1012 DP @ 800°C and induction tempered at 200°C for 1h (base metal)

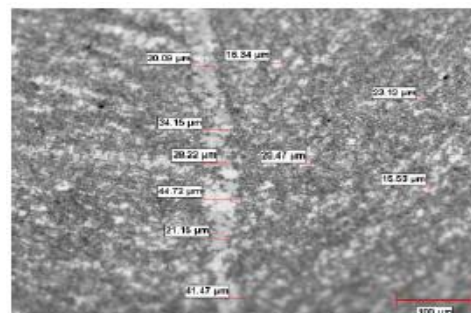


Fig 16. Ferrite band width/Grain size at the weld region and HAZ of SAE 1012 M DP@ 740°C sample

Microstructures clearly show the ferrite-pearlite structure in the ‘as drawn’ state and ferrite-martensite structure in the DP treated conditions. In all conditions the weld line is clear with a white band along the weld line indicating lower carbon content. The continuity of the rolling lines is interrupted at the weld region. This weld line is essentially ferrite and it seems that carbon diffusion has occurred at.

The weld juncture due to the high heat generated at the weld interface. The decarburization is clearly visible in Fig.14 (a). Also the HAZ seems to be rich in carbon or having more accumulation of martensite(fig.16). DP treatments carried out up to 810°C was clearly ineffective in the weld region with no ferrite- martensite structure. The fact that the torsion tested samples has always failed along the weld indicates that the ferrite band is the weakest region susceptible for failure. The clear inhomogeneity in the weld and HAZ can initiate a crack at this juncture during cyclic loading.

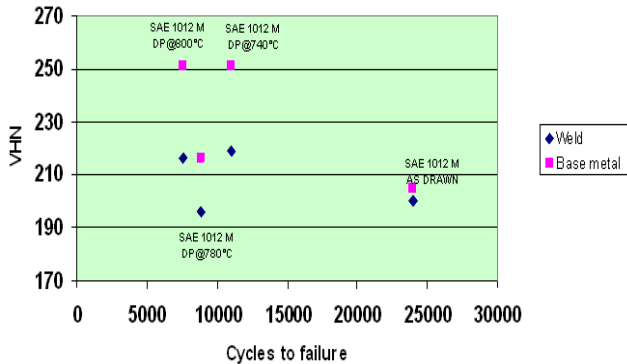


Fig.17. Hardness Vs Distance plot across weld section

A decrease in hardness was always found in the weld region irrespective of whether the material is DP treated or not. This is due to the excessive ferrite concentration in the weld region. The hardness as well as the difference in hardness was found to increase with the DP treatment. As-drawn sample showed the least difference in hardness which had given maximum torsional fatigue life.

V. CONCLUSIONS

The SEM analysis showed inclusions at several micro crack initiation sites which have led to the final fracture through weld line. It appears as if the crack has initiated at the interface of the matrix and inclusions which mainly included aluminium and calcium silicates, Titanium impurities and some oxides. Failure of SAE1012 DP@740°C at 6500 cycles is attributed to its in homogeneity due to the structural distinction of base metal and weaker weld region. Presence of silicates and chlorides in the weld region might have initiated the fracture.

There is marked difference in the grain size between grains at the weld region and base metal. The ferrite band grain size were almost double than the base metal grain size. Among the as drawn specimens with ferrite pearlite structure, difference in hardness between the weld region and base metal is less for all samples which is the reason for its high performance of 25000 cycles. Presence of silicates has initiated the fracture in this case also. Microstructural analysis of all SAE 1012 samples shows clear demarcation in the weld region compared to the base metal. The regular rolling lines in the circumferential direction is seen to have a clear discontinuity along the weld line. This weld line on close observation is seen as white ferrite band in the ferrite-martensite background. Failure have occurred through the weld line in all cases though the cycles to failure have varied. The white band in the weld region may be due to the carbon diffusion which have occurred due to the high

temperature at the seam during welding process. The grain size is also slightly bigger at the weld line.

Among the tested samples, SAE1012 ‘as drawn’ sample with ferrite pearlite structure showed more torsional fatigue strength compared to other samples with ferrite-martensite structure.

REFERENCES

1. M. Wan, S. N. Yie, M. T. Jahn and S. M. Kuo “Studies on the stress-strain relations of dual-phase steels”, Journal of Materials Science, Volume 16, Number 10 / October, 1981
2. www.worldautosteel.org/steeltypes/properties
3. M.Tayanc, A.Aytac, A.Bayram “The effect of carbon content on fatigue strength of dual-phase steels Journal of Materials and Design” April Vol 28, Issue 6 Pages 1827–1835, 2007
4. Zhonghao Jiang, Zhenzhong Guan and Jianshe Lian ,”The relationship between ductility and material parameters for dual-phase steel”, Journal of Materials Science, Volume 28, Number 7 / January, 1993
5. Gerald Weimer, Ray Cagganello, “Electric Resistance Welding at a Glance: Process, Power Supply, and Weld roll basics” TPJ - The Tube & Pipe Journal@ June 13, 2002
6. Karl-Heinz Brenzing, Dusseldorf, “Steel tube and pipe manufacturing process” www.smrw.de/files/steel_tube_and_pipe.pdf
7. C. M. Wan, K. C. Chou, M. T. Jahn and S. M. Kuo, “Fatigue studies on dual-phase low carbon steel”, Journal of Materials Science, Volume 16, Number 9 / September, 1981
8. A. N. Tkach, N. M. Fonshtein, V. N. Simin'kovich, A. N. Bortsov and Yu. N. Lenets, “Fatigue crack growth in a dual-phase ferritic-martensitic steel”, Journal of Materials Science, Volume 20, Number 5 / September, 1985
9. K. K. Chawla, P. R. Rios and J. R. C. Guimarães, “Fractography of a dual phase steel” Journal of Materials Science Letters, Volume 2, Number 3 / March, 1983